INPUT IMPEDANCE MEASUREMENTS OF DISK CONE ANTENNAS

Thesis for the Degree of M. S.

MICHIGAN STATE COLLEGE

Harry DeVere Ruhl, Junior

1952

This is to certify that the

thesis entitled

INPUT IMPEDANCE MEASUREMENTS

OF DISK CONE ANTENNAS

presented by

Harry DeVere Ruhl, Junior

has been accepted towards fulfillment
of the requirements for

M.S. degree in Physics

Robert D. Spence
Major professor

Date August 15, 1952

O-169

INPUT IMPEDANCE MEASUREMENTS OF DISK CONE ANTENNAS

By

Harry DeVere Ruhl, Junior

A THESIS

Submitted to the School of Graduate Studies of Michigan State College of Agriculture and Applied Science in partial fulfillment of the requirements for the degree of

MASTER OF SCIENCE

Department of Physics and Astronomy

1952

10-14-52 (3)

TABLE OF CONTENTS

ACKNOWLEDGMENTS

I wish to express my sincere thanks to Dr. Alfred Leitner and Dr. Robert D. Spence for their suggestions and assistance. I am also greatly indebted to Mr. Charles Kingston for his aid in construction details and to Mr. Robert Gault and Mr. Albert Smith for their help in photographic work.

H D Budd, Jr.

INTRODUCTION

The purpose of this thesis was to determine the input impedance of a disk cone antenna. The configuration in this experiment was a circular disk of finite extent as the ground plane, and a circular cone of wide angle with a flat base. The cone was located with its apex at the center of the disk and its axis coincident with the axis of the disk. See Figure 1.

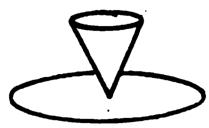

Figure 1

The disk cone antenna belongs in a family generally known as conical antennas. S.A. Schelkunoff[12] in his book, "Electromagnetic Waves", considered and solved the problem for cones having half angles of less than two degrees. In later papers[13,4], Schelkunoff indicated a method of solution for the problem involving wide angle cones having spherical caps, from which P.D.P. Smith[15] obtained an approximate solution. Both of these solutions are obtained for symmetrical biconical antennas, two cones having the same axis and touching at the apices. The impedance values found by these authors are twice the impedance of one cone perpendicular to, and with its apex touching, an infinite ground plane. The configuration of the disk cone, therefore, most nearly approaches that of Smith's work, with these exceptions: the ground plane, which is finite in the disk cone, and the base of the cone, which in Smith's paper had a spherical cap and in this experiment was flat.

Figure 2.

Five of the cones used. Beginning at the extreme right and proceeding clockwise the cones have half angles of 60°, 50°, 15°, 30°, and 45°. All cones have a slant height of $\lambda/4$.

METHOD OF CALCULATION

The method of determining the impedance of the antenna consisted of using it as the termination of a transmission line and measuring the terminating impedance.

In using this method two quantities must be accurately measured;

1. The standing wave voltage ratio defined as

$$\rho = \frac{\text{Voltage Maximum}}{\text{Voltage Minimum}} . \qquad (1)$$

2. The distance of the first voltage minimum from the terminal impedance. (x_{min})

The terminal impedance is then given by

$$Z_T = Z_{Ant} = Z_0 \frac{(1 - j\rho \operatorname{Tan} \beta x_{min})}{(\rho - j \operatorname{Tan} \beta x_{min})} , \qquad (2)$$

where $\beta = \frac{\omega}{c} = \frac{2\pi f}{c} = \frac{2\pi}{\lambda}$, and where Z_0 is the characteristic impedance of the line.

$$Z_0 = \frac{60}{\sqrt{\varepsilon_r}} \ln \frac{b}{a} , \qquad (3)$$

where ε_r is the dielectric coefficient. Z_0 was equal to 79.2 ohms for the transmission line used.

The theoretical consideration of this antenna assumes that it is located in free space. This is difficult in practice, but it is possible to place the antenna sufficiently far from surrounding objects so that they will have very little effect. However, in doing this, some attenuation was introduced in the transmission line.

For lines of small attenuation the phase constant (β) is for practical purposes the same as that of a dissipationless line, hence the shift of the first minimum remains the same. The standing wave ratio is always decreased by attenuation, and the effect is greater for large standing wave ratios as shown below. The coefficient of attenuation (α) was computed, and corrections were then made in the standing wave ratio, in the following manner. For coaxial lines,

$$\alpha = \frac{1}{2}\sqrt{\frac{f\mu\pi}{\sigma}}\sqrt{\frac{\varepsilon_0}{\mu_0}}\;\frac{1}{\ln\frac{b}{a}}\left(\frac{1}{b}+\frac{1}{a}\right), \qquad (4)$$

f = frequency = 2.82×10^9 cycles/second,

σ = conductivity of metal = 1.55×10^7 mho/meter,

b = radius of outer conductor = 1.19×10^{-2} meters,

a = radius of inner conductor = $.318 \times 10^{-2}$ meters,

μ = $1 \times 4\pi \times 10^{-7}$ henrys/meter,

μ_0 = $4\pi \times 10^{-7}$ henrys/meter,

ε_0 = $10^{-9}/36\pi$ farads/meter.

The conductivity used here is an average value of that for brass. No information being available for brass tubing and rod used, an average was taken over those values found in reference books[6,7], which was

$\sigma_{brass} \doteq .25\,\sigma_{copper}$. The attenuation was then found to be $\alpha \doteq .0107$ nepers/meter.

Voltage maxima in the standing wave pattern on a transmission line occur whenever the incident and reflected waves are in phase, and minima whenever they are 180° out of phase. Hence the standing wave ratio may be expressed as

$$\rho = \frac{|V_I| + |V_R|}{|V_I| - |V_R|}, \tag{5}$$

where $|V_I|$ is voltage of the incident wave and $|V_R|$ is the voltage of the reflected wave.

Since the units of voltage are arbitrary, $|V_I|$ may be taken as unity and the value of $|V_R|$ calculated from the measured value of ρ. Since the reflected wave has traveled from the detector to the antenna and back again, it has been attenuated by a factor of $\varepsilon^{-\alpha d}$, where d is twice the distance from the detector to the antenna. In the present experiment, $d \doteq 4.27$ meters, $\alpha d \doteq .0457$. We designate the value of the reflected voltage which would have been present without attenuation as $|V_R'|$. It is seen that $|V_R'| = |V_R|\ \varepsilon^{\alpha d}$ and we find that $|V_R'| \doteq 1.05|V_R|$. This value is substituted in equation (6) and the corrected standing wave ratio ρ' is used to calculate the antenna impedance:

$$\rho' = \frac{|V_I| + |V_R'|}{|V_I| - |V_R'|} \tag{6}$$

where $|V_I| = 1$.

From equation (5) we find that large standing wave ratios occur when $|V_R|$ is large. From the development leading to equation (6) we find that $|V_R'| = 1.05\,|V_R|$, so that the difference between $|V_R'|$ and $|V_R|$ is greater for large standing wave ratios. Since in equation (6) we add $|V_R'|$ to $|V_I|$ in the numerator, and subtract it from $|V_I|$ in the denominator, ρ' is always larger than ρ . The difference increases with larger standing wave ratio.

The detector was located about twenty wave lengths from the terminal of the transmission line. The shift of the first minimum was determined by measuring the shift of the 41st minimum, the two being essentially identical. Actually, three or four minima and four maxima could be observed in a slotted section of the transmission line, both with a shorted terminal and with an antenna. Altogether, eight values of the shift were observed, and each reading was repeated several times. Separate observations of standing wave ratios, voltage maximum to adjacent voltage minimum, were also taken, and then repeated. As a check, the sets of readings were repeated and averages were taken over all readings. Finally the standing wave ratio was corrected in accordance with equation (6).

OPERATING CONDITIONS

A wave length of approximately ten centimeters was chosen primarily for three reasons;

1. It was short enough so that surrounding objects were electrically far enough away so as to have very little effect. (20 λ or more)
2. It was large enough so that component parts could be machined while still maintaining necessary tolerances.
3. The antenna could be small enough so that no framework was needed to support the cone.

The antenna was fed by a coaxial line, the outside conductor ending in the disk and the center conductor supporting the cone. It was necessary therefore to have an aperture at the center of the disk and the apex of the cone could not be a point, so the field configuration was somewhat different from the theoretical problem. Since it was necessary to place the antenna at some distance from all other equipment, the coaxial line of considerable strength was needed. The outside conductor was therefore made of 1" brass tubing, and the inside conductor of 1/4" brass rod. Styrofoam was used as a spacing material, in order to keep the conductors concentric and yet not introduce any appreciable error by changing the dielectric constant. Polystyrene spacers were used at two places along the transmission line where either the outer conductor was made larger or the inner conductor was made smaller so that the characteristic impedance of the line remained a constant.

Near the terminal of the transmission line both the inside and outside conductors were tapered so that the aperture in the disk could be as small as possible. See Figure 3 . The ratio of the two radii was kept constant along the tapered section, thus maintaining a constant characteristic impedance. This was checked by independently shorting both ends of the tapered section and observing the resulting standing wave patterns which were found to be the same in both cases.

Tapered Section And Termination

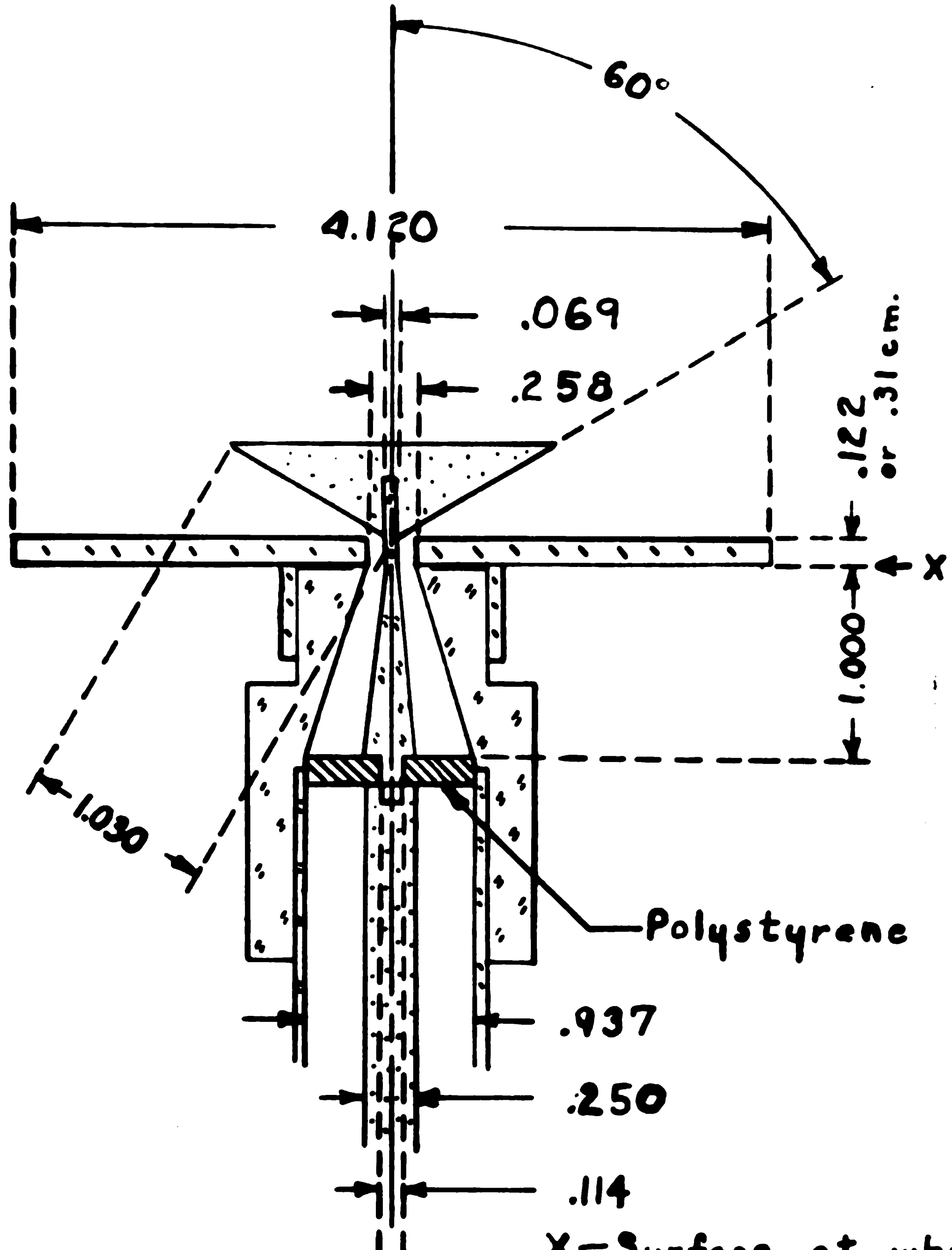

X—Surface at which
short was made

Cone
Half Angle 60°
Slant Height λ/4

Ground Plane
Radius λ/2

Scale 1" = 1"

Figure 3

EQUIPMENT

The oscillator was the resonant cavity type employing a 2C40 "light house" tube. It was modulated by a "square wave" pulse at a frequency of approximately eight hundred cycles per second using a multivibrator, shaper, and modulator circuit, as in Figures 6 and 7. The multivibrator circuit was conventional, using a 6SN7 dual triode, and drove a 6V6 tube from saturation to cut-off, giving a "square wave" output. The modulating unit used three 6L6 tubes in parallel. The screen grids and plates of the 6L6 tubes were connected together. This reduced the resistance of these tubes, and resulted in larger voltages from the plate to the cathode of the 2C40 tube. Two separate regulated power supplies with separate grounds were used, one for the modulator and oscillator, and one for the multivibrator and shaper. The oscillator was placed in parallel with the cathode resistor of the 6L6 tubes, and the 6L6 tubes in turn were driven by application of the "square wave" voltage. This drove them from near cut-off to saturation. As a result, a square wave voltage of approximately two hundred volts was applied between the cathode and the plate of the oscillator. Since the characteristics of the 2C40 tube show that oscillation ceases at plate voltages below 75 volts[18], the oscillator was pulse modulated.

Energy was taken from the cavity by a probe connected to the large coaxial line by way of a flexible coaxial line. The two coaxial sections were matched by double stub tuning, as shown in Figure 11.

Energy was extracted by a thin probe which traveled along a slotted section of the coaxial transmission line. The probe was inserted into the line a very small distance to insure loose coupling and minimize the discontinuity it presented.

The probe was connected to the center conductor of the detector unit, Figure 12, and could be raised or lowered into the main coaxial line. A moveable short was located in the detector unit between the center and outer conductor, with its position adjustable so it could be tuned to give a maximum of energy detected. A crystal was located perpendicular to, and between, the probe and short to detect the radio frequency energy. Essentially, the equivalent circuit was as shown below.

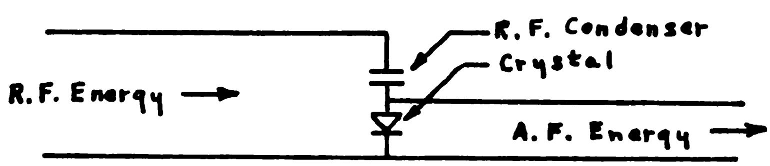

Figure 4

Crystals have a square law response to voltage and since the voltage along the line, when shorted, varies as $\sin \beta x$, the detected signal should vary as $\sin^2 \beta x$. (x being the distance from the terminal end) The crystal was calibrated by placing a short at the terminal and plotting voltage vs. distance, then comparing this with a $\sin^2 \beta x$ curve. These curves, as shown in Figure 13 corresponded so closely that the meter in the amplifier, which was designed and calibrated to operate in conjunction with a square law detector, could be used to read standing wave voltage ratio. Actual voltage units were not important since they were used in a ratio. Minima and maxima were located by use of the same meter. A battery operated preamplifier, Figure 14, was used close to the probe to raise the signal level before noise was introduced.

Block Diagram of the Experimental Equipment

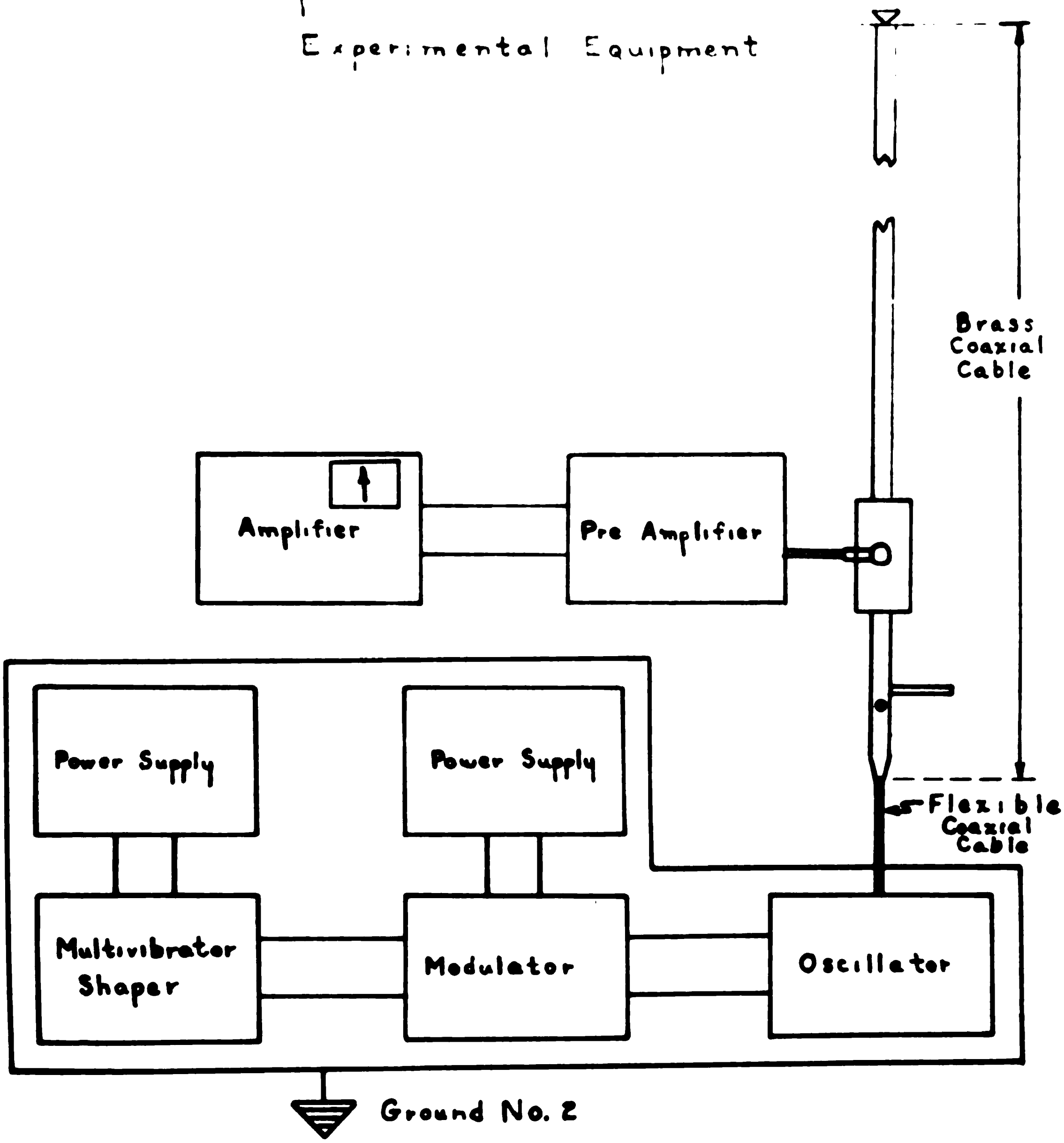

Figure 5

Multivibrator and Shaper

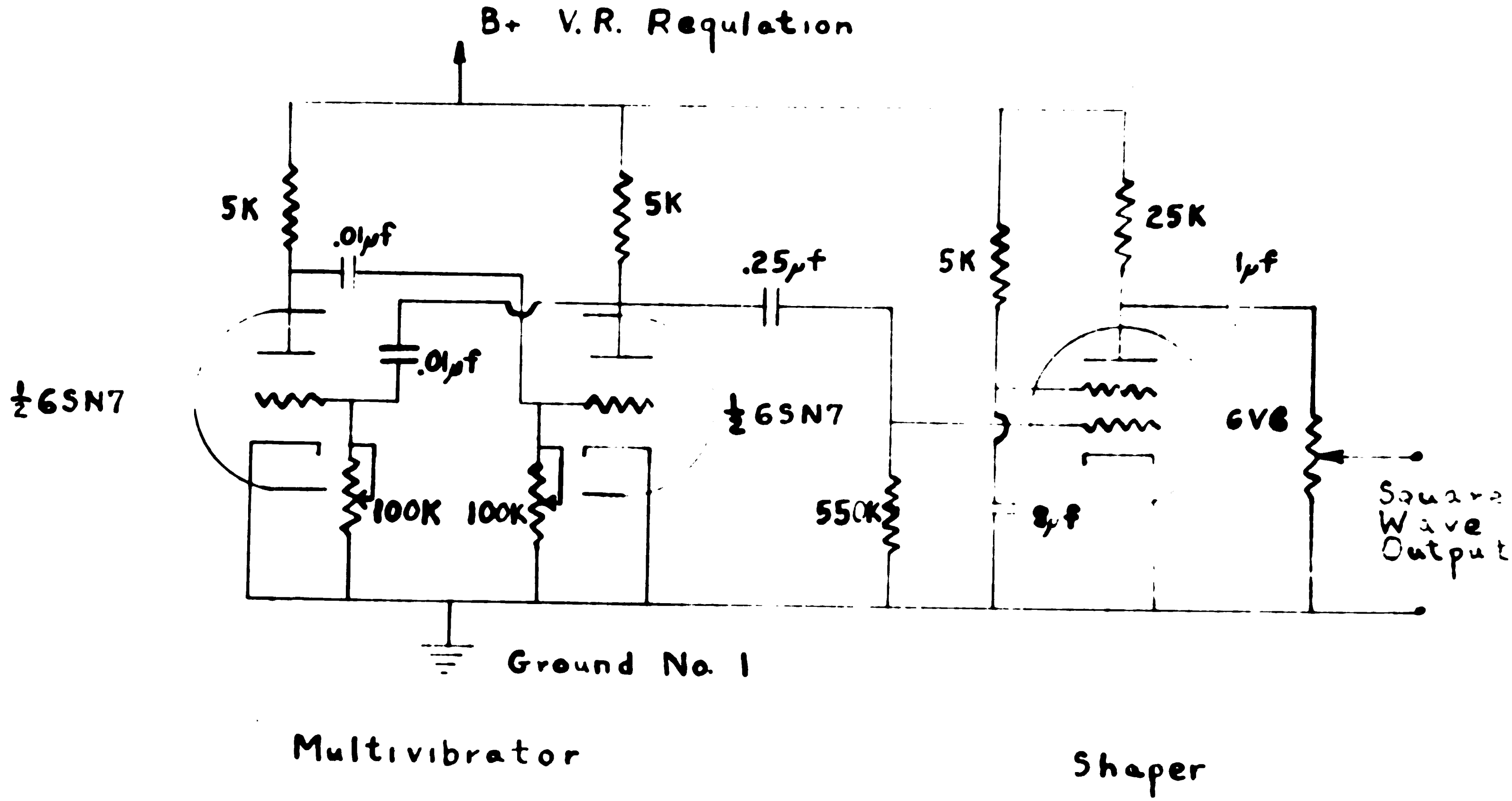

Figure 6

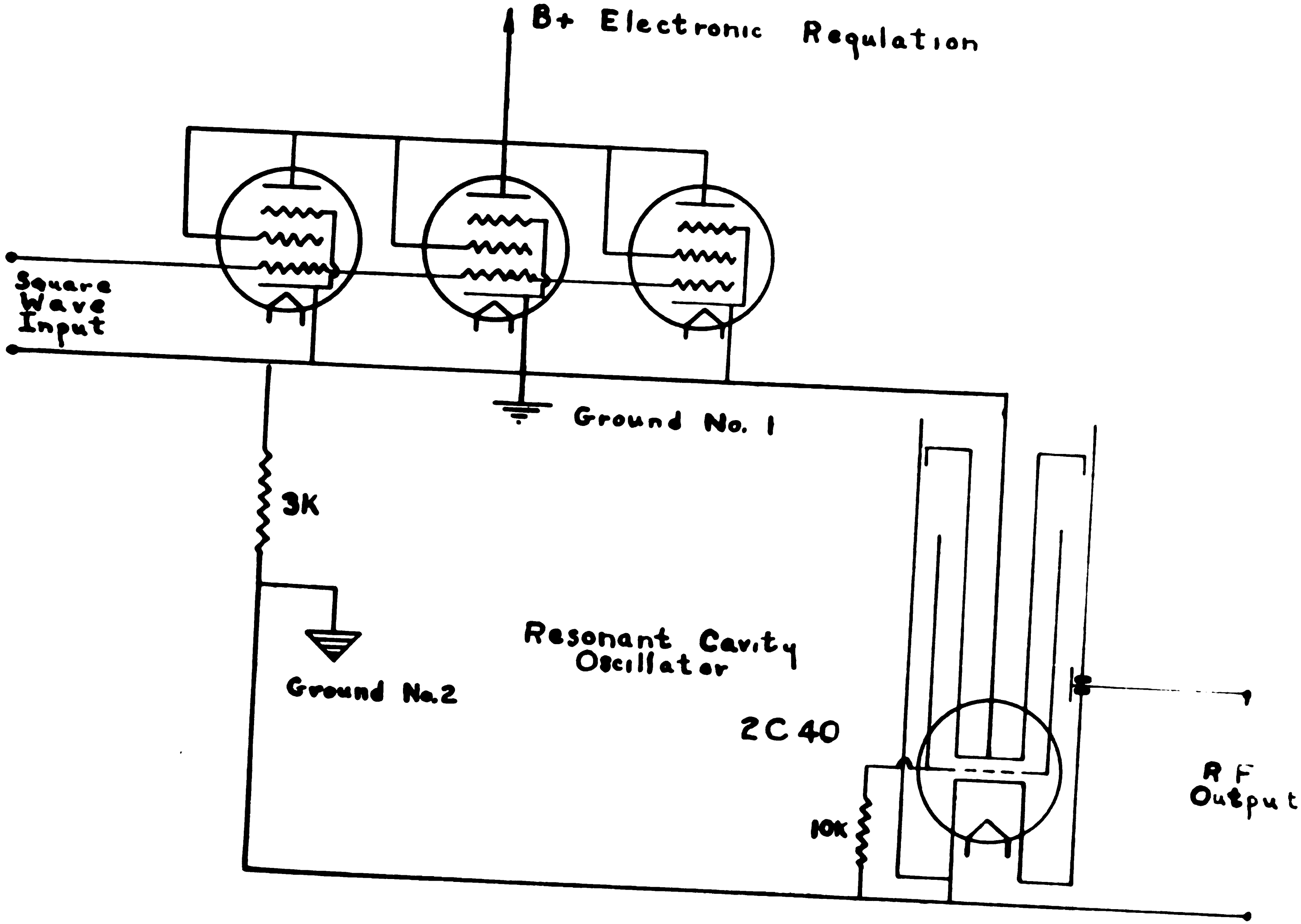
B+ Electronic Regulation
Square Wave Input
Ground No. 1
3K
Ground No.2
Resonant Cavity Oscillator
2C40
10K
RF Output

Figure 7

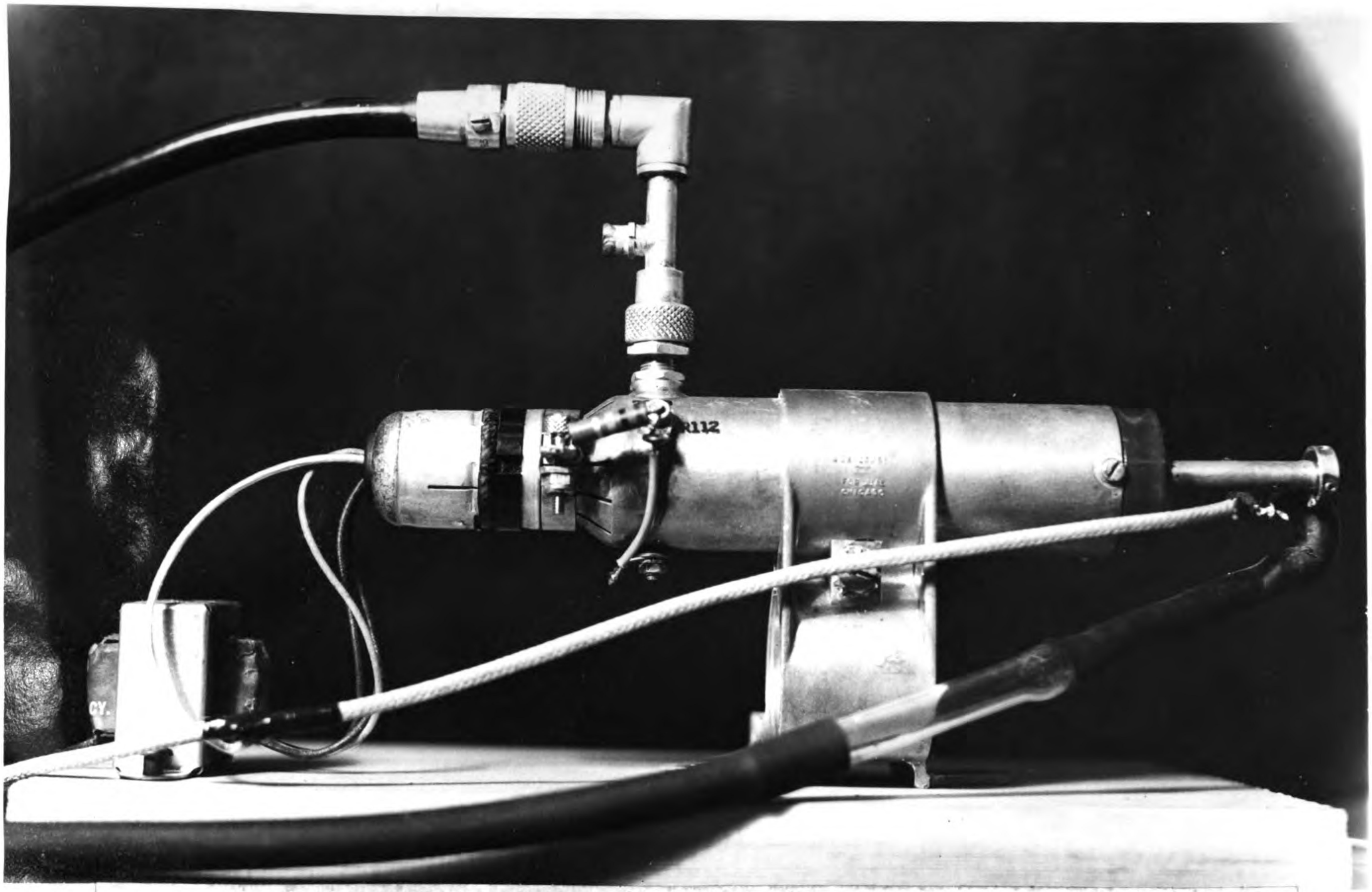

Figure 8.
The resonant cavity oscillator. It was air cooled by way of the rubber tube having a glass section. The connections at the extreme right and left ends of the cavity were from the modulator. At the top was the connection to the probe and the flexible coaxial line.

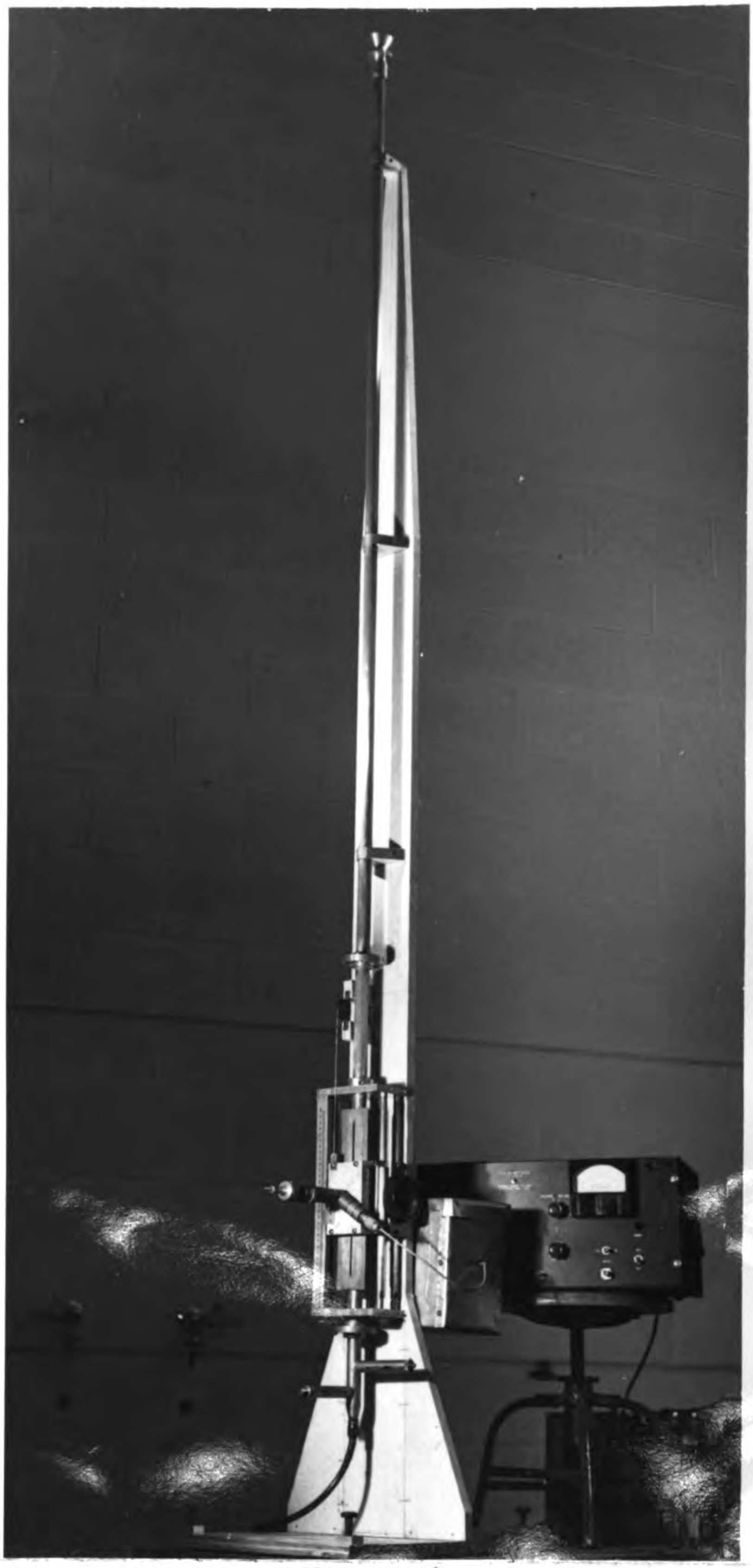

Figure 9.
The experimental equipment showing flexible coaxial line, brass transmission line, antenna, detector, and amplifiers.

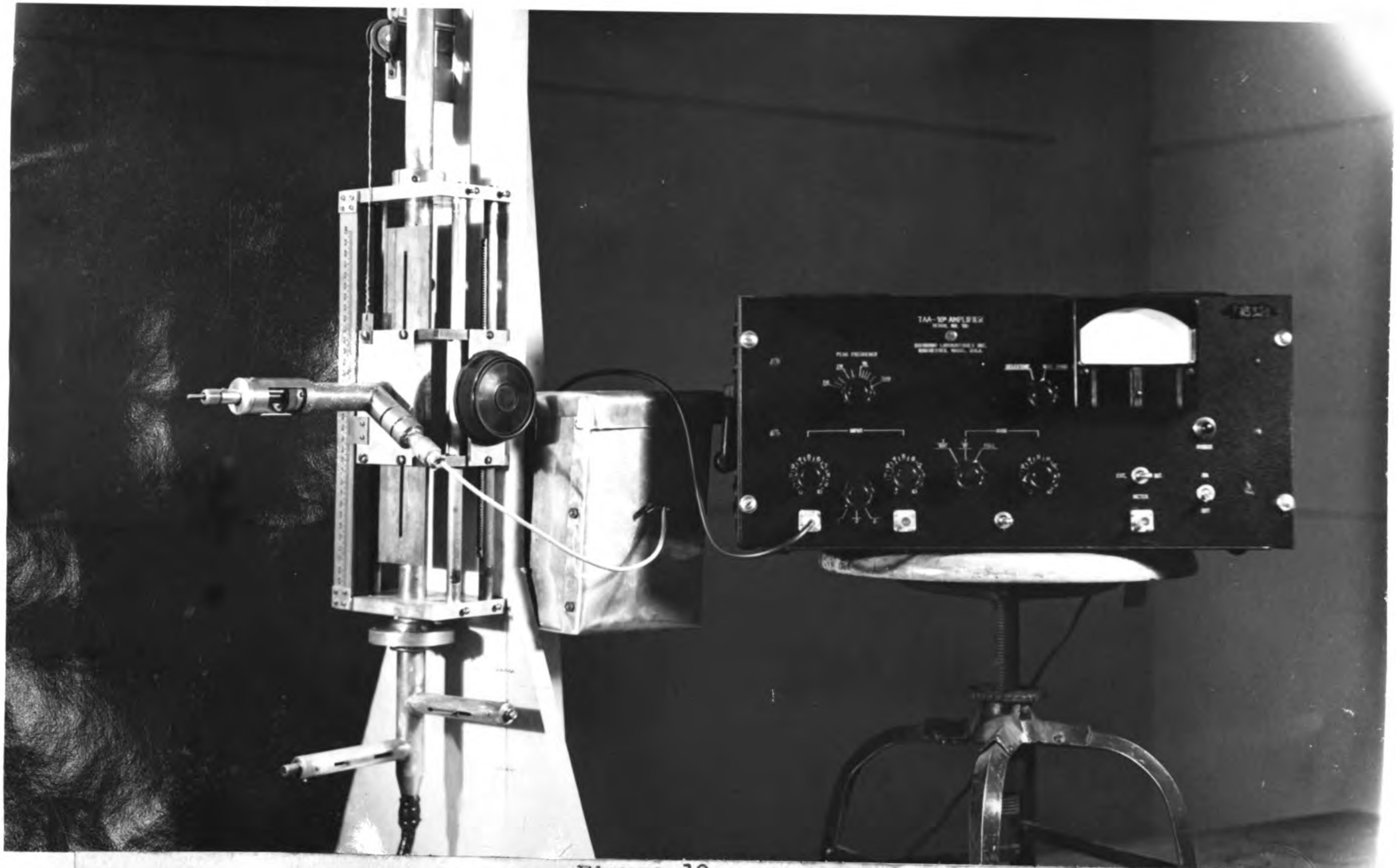

Figure 10.

The equipment used to determine the standing wave pattern. From left to right the standing wave detector, the slotted section, the container for the pre-amplifier, the main amplifier, and meter from which the readings were taken.

Matching Stub

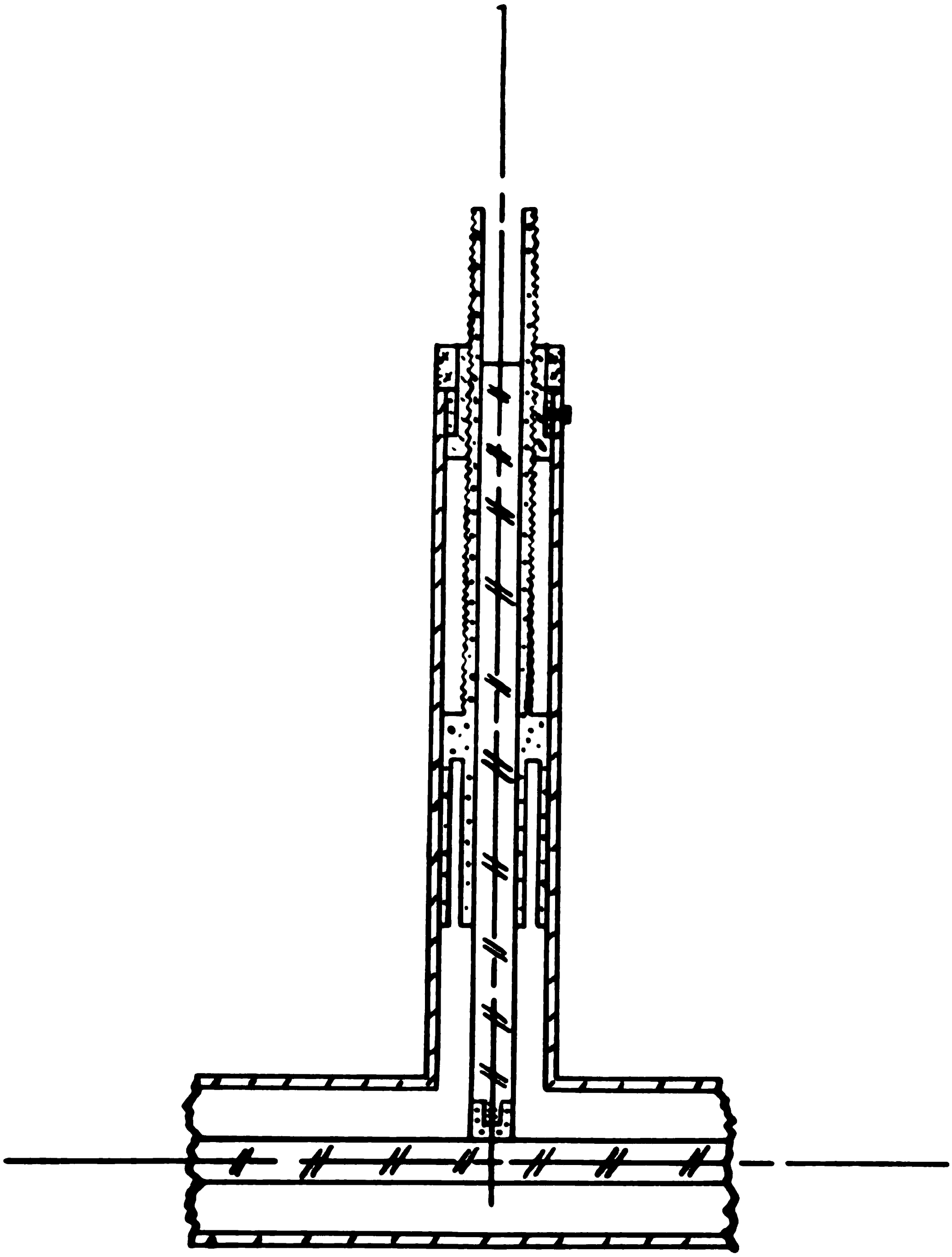

Two Stubs Used, Separated 1.5" At Their Centers

Figure 11

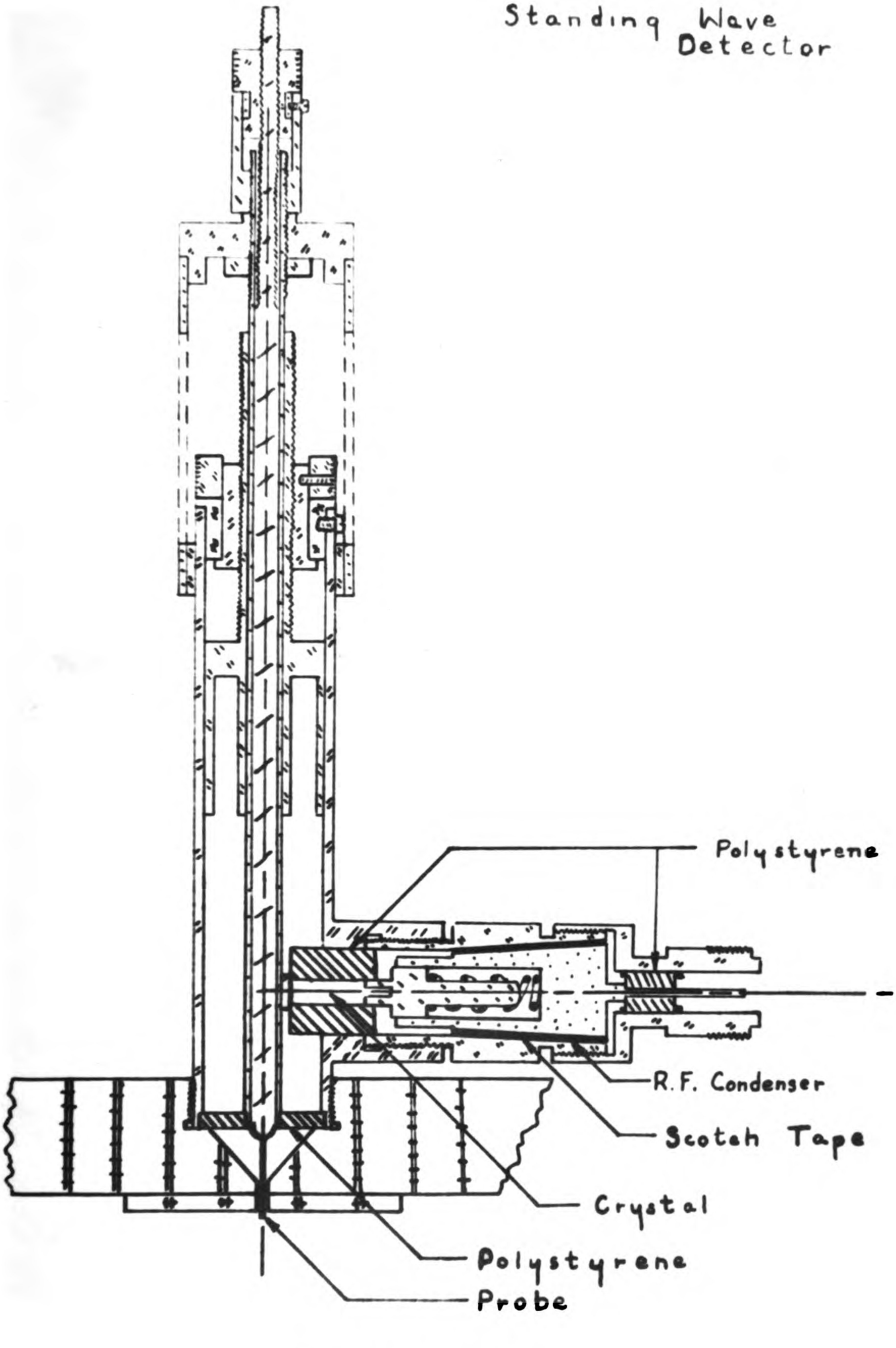
Standing Wave Detector
Polystyrene
R.F. Condenser
Scotch Tape
Crystal
Polystyrene
Probe

Figure 12

Typical Crystal Calibration Curve Compared With a $\sin^2 \beta x$ Curve

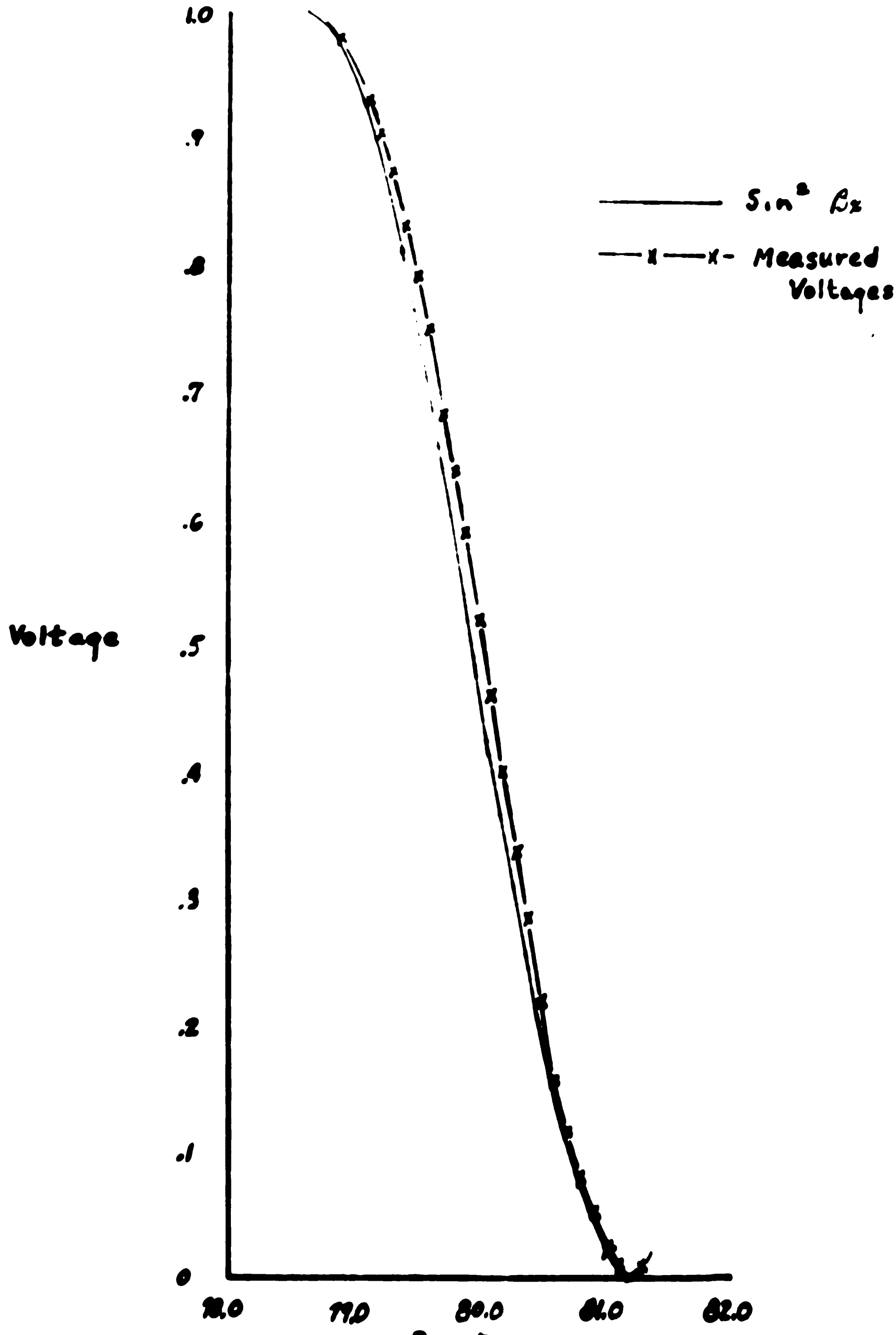

Figure 13

Pre-Amplifier

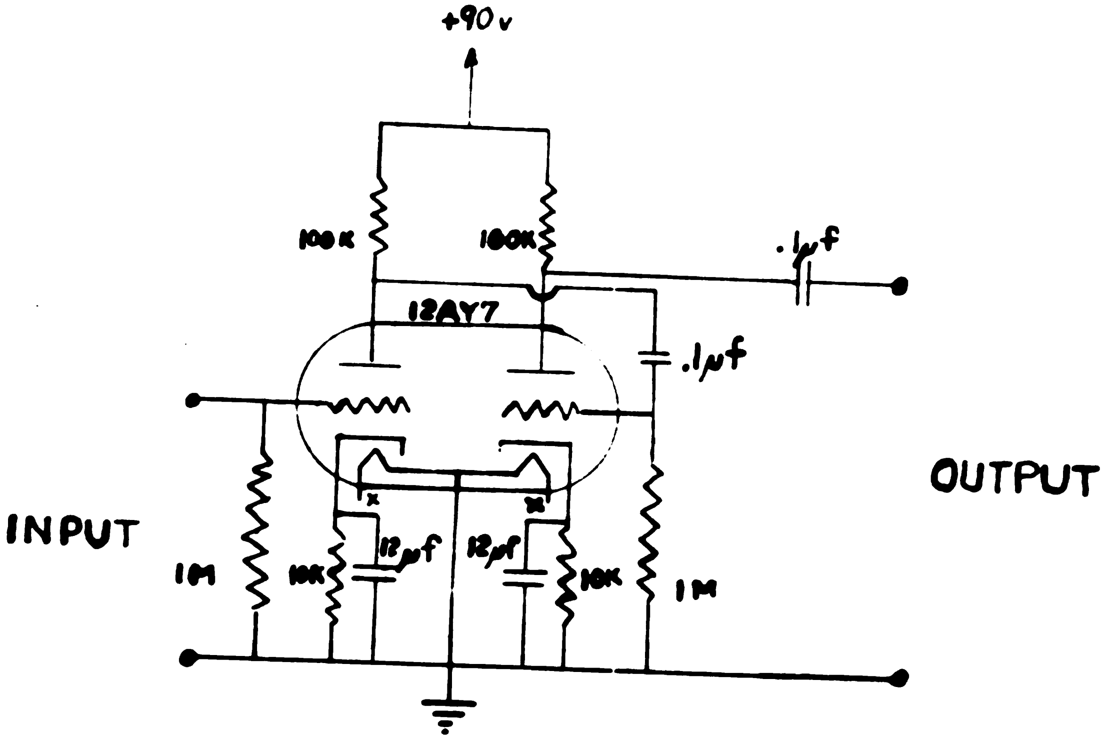

All Voltages Battery Supplied

Figure 14

SOURCES OF ERROR

There are several sources of error present, which come under five main headings.

Concentricity of Conductors

The inner conductor was held concentric by using styrofoam spacers. These were observed to contribute no detrimental effect by comparing the curves obtained when the end was shorted with and without the spacers. The effect of the single polystyrene spacer between the detector and the termination was checked in the same manner and found to contribute no observable effect.

The dielectric coefficient ε_r of polystyrene is 2.55[19]. As a consequence, when it was used as a spacer, the inner conductor had to be undercut, or the outer conductor increased in size, to maintain the characteristic impedance of the line constant, cf. equation (3). When styrofoam was used as a spacer, it was found unnecessary to change the conductor sizes. Styrofoam, being such a large percentage of air by volume, has a dielectric constant essentially equal to one, rendering changes of conductor sizes unnecessary.

Another precaution taken to maintain the center conductor concentric was to mount the entire brass section of the transmission line vertically. The line was maintained vertical by leveling screws, and as indicated, by the use of a level.

Attenuation

The attenuation due to the conductivity of brass has already been computed and corrected for, see page 5. The spacers used to keep the center conductor concentric were unavoidable and probably contributed a negligibly small additional amount to the attenuation. The ratio of conductor sizes was very nearly the ratio giving minimum attenuation.

Calibration of the Crystal

This may introduce some error, though small, as indicated previously. See page 13.

Discontinuities

Several of the discontinuities are unavoidable. The probe, the slot, the spacers, etc. were all necessary, but once again, the smoothness of the curve representing the standing wave pattern when the termination was a short indicated the minuteness of their contributions. The probe was inserted in the line a very small distance to minimize its effect.

Measurements

The errors in the location of the positions of maximum or minimum voltage were greatest for small standing wave ratios. As shown in Figure 15, for small standing wave ratios the minima and maxima appear much wider than they do for large standing wave ratios. As a consequence the exact positions of maxima and minima were more difficult to locate, and greater errors were introduced when the standing wave ratios were small.

The errors in reading standing wave ratios were greatest for large standing wave ratios. Figure 15 shows that a small error in the location of minima or maxima give larger deviations from the true stationary value of voltage when standing wave ratios are large. This effect is due to the shape of the curve of voltage vs. distance along the transmission line. The error introduced by attenuation, as discussed on p. 5, has a similar effect. It is not related to the error due to the shape of the curve.

Both of these effects were minimized by carefully making a large number of observations and taking an average.

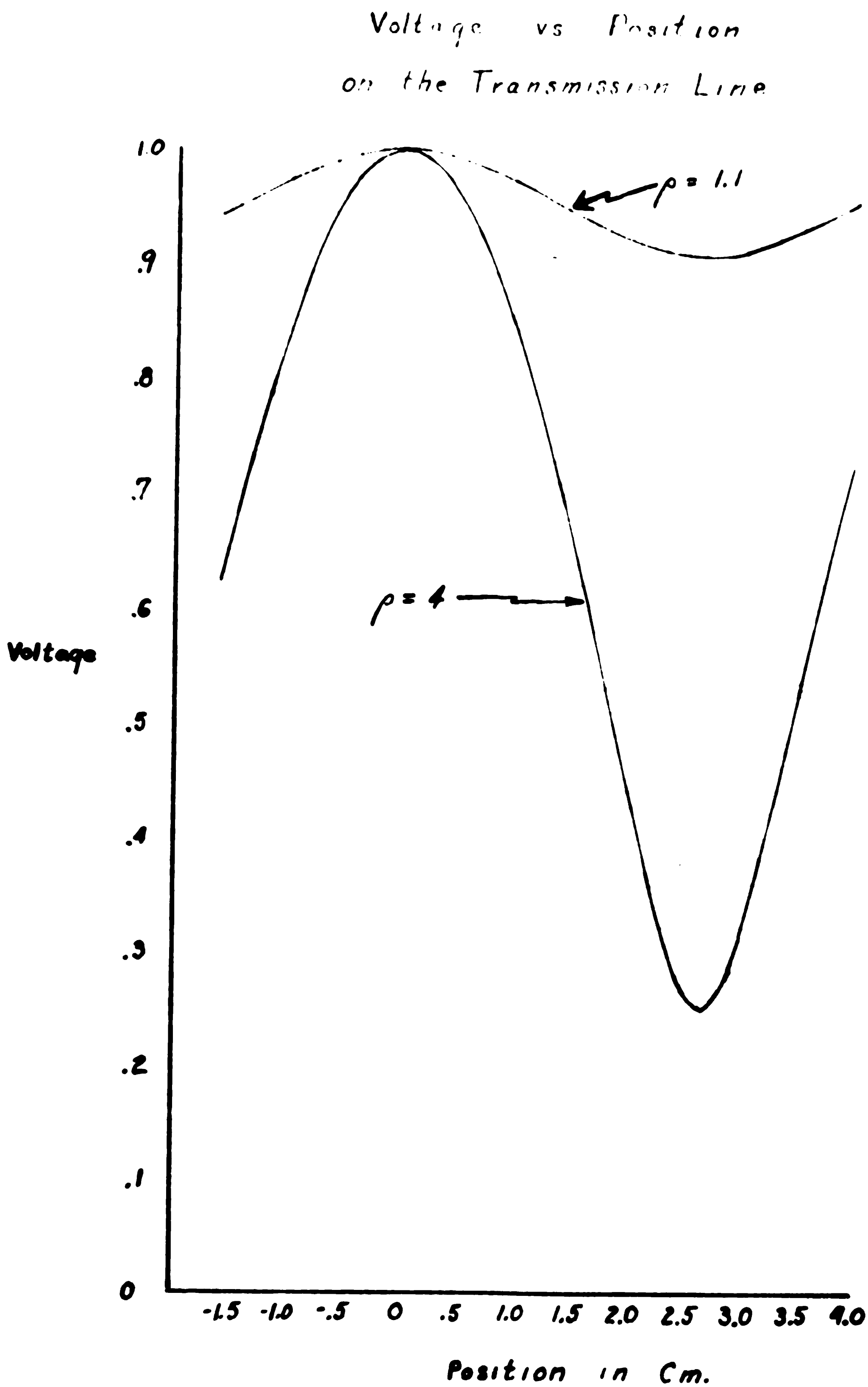
Voltage vs Position
on the Transmission Line
1.0
.9
.8
.7
.6
.5
.4
.3
.2
.1
0
Voltage
ρ = 1.1
ρ = 4
-1.5 -1.0 -.5 0 .5 1.0 1.5 2.0 2.5 3.0 3.5 4.0
Position in Cm.

Figure 15

SAMPLE CALCULATION

Readings of Position in Centimeters

Short as Termination*		Antenna as Termination	
Minima	Maxima	Minima	Maxima
91.65	88.97	87.11	89.73
.31	.96	.14	.72
91.96	.93	.11	.68
	.92	.11	.70
	.96	.14	.69
	.91	.14	.70
	.91	.11	.73
	.96	.12	.71
	.92	.12	.72
	88.94	.13	.70
	.31	87.12	89.71
	89.25		
86.34	83.69	81.80	84.46
.31	.65	.79	.42
86.65	.68	.79	.42
	.68	.78	.43
	.67	.81	.40
	.65	.79	.42
	.66	.81	.43
	.70	.79	.40
	.70	.79	.41
	.69	.79	.43
	83.68	81.79	.43
	.31		84.42
	83.99		

* .31 centimeters was added to the averages of readings taken when the termination was a short, in order to correct for the thickness of the ground plane. See Figure . This correction was added because high readings are towards the termination.

Minima	Maxima	Minima	Maxima
81.02	78.38	76.50	79.20
.31	.41	.50	.14
81.33	.41	.49	.20
	.43	.49	.20
	.38	.50	.18
	.39	.46	.19
	.36	.48	.17
	.44	.47	.15
	.38	.50	.16
	.40	.48	.14
	78.40	76.49	79.17
	.31		.
	78.71		

75.70	73.10	76.50	73.85
.31	.10	.50	.95
76.01	.06	.49	.81
	.00	.49	.86
	.07	.50	.80
	.11	.46	.90
	73.00	.48	.80
	.02	.47	.89
	.05	.50	.79
	72.98	.48	.76
	73.05	76.49	73.84
	.31		
	73.36		

<u>Readings of Standing Wave Ratio</u>

3.8	3.8	3.7	3.8	3.9	3.7
.7	.8	.7	.8	.9	.7
.7	.8	.7	.8	.9	.8
.7	.8	.7	.7	.8	.7
.8	.8	.7	.7	.9	.8

Total 112.9 for 30 readings. Average 3.76

Correction for Standing Wave Ratio

$$\rho = \frac{|V_I| + |V_R|}{|V_I| - |V_R|} = 3.76 = \frac{1 + |V_R|}{1 - |V_R|} \qquad |V_R| = \frac{2.76}{4.76} = .580 \text{ voltage units}$$

$$|V_R'| = 1.05\,|V_R| = 1.05 \times .580 = .609 \text{ voltage units}$$

$$\rho' = \frac{|V_I| + |V_R'|}{|V_I| - |V_R'|} = \frac{1.609}{.391} = 4.11$$

Shift of the Standing Wave Pattern

	Short	Antenna
Minimum	91.96	
Maximum	89.25	89.71
Minimum	86.65	87.12
Maximum	83.99	84.42
Minimum	81.33	81.79
Maximum	78.71	79.17
Minimum	76.01	76.49
Maximum	73.36	73.84

Shifts of (X_{min}) in Centimeters

4.86	4.86
4.85	4.82
4.89	4.84
4.86	4.87
4.86	4.92
4.84	4.85
4.84	4.93
4.84	4.86
4.83	4.83

Total 87.45 for 18 readings.
Average 4.86 cm.

Solution of the Problem

$$Z_T = Z_0 \frac{1 - j\rho \operatorname{Tan} \beta x_{min}}{\rho - j \operatorname{Tan} \beta x_{min}}$$

$$\beta x_{min} = \frac{2\pi x_{min}}{\lambda} = \frac{2\pi 4.86}{10.64} = .913\pi = 164^\circ 18'$$

$$\operatorname{Tan} \beta x_{min} = -.281$$

$$\rho \operatorname{Tan} \beta x_{min} = 4.11 \times (-.281) = -1.15$$

$$Z_T = 79.2 \frac{1 + j1.15}{4.11 + j.281}$$

$$= \frac{79.2 \times 1.53 \angle 48^\circ 49'}{4.12 \angle 3^\circ 57'}$$

$$= 29.4 (.709 + j.705)$$

$$Z_T = (20.8 + j20.7) \text{ ohms}$$

RESULTS AND CONCLUSIONS

It should be noted that for the disk cone antenna, there are three quantities which may be varied: the half angle of the cone, the slant height of the cone, and the radius of the ground plane, The results of these variations are shown in the accompanying graphs.

The variations in the input impedance due to changes of slant height shown in Figure 16 indicate in a very general way what happens. The resistance component appears to dip in the vicinity of $3/4\ \lambda$. Actually too few points were taken to give a conclusive picture.

The reactive part represented a far more interesting variation. The reactance was inductive when the slant height was an odd multiple of quarter wavelengths, and capacitive at even multiples of a quarter wavelength. These variations indicated some point of resonance between each change of one quarter wavelength. Exact locations of these points are not known because intermediate slant heights were not observed.

The similarities and differences between the conical antenna as computed by P.D.P. Smith and the disk cone have already been discussed on page 1. For purposes of comparison the results of his

Impedance Variation as Slant Height Changes

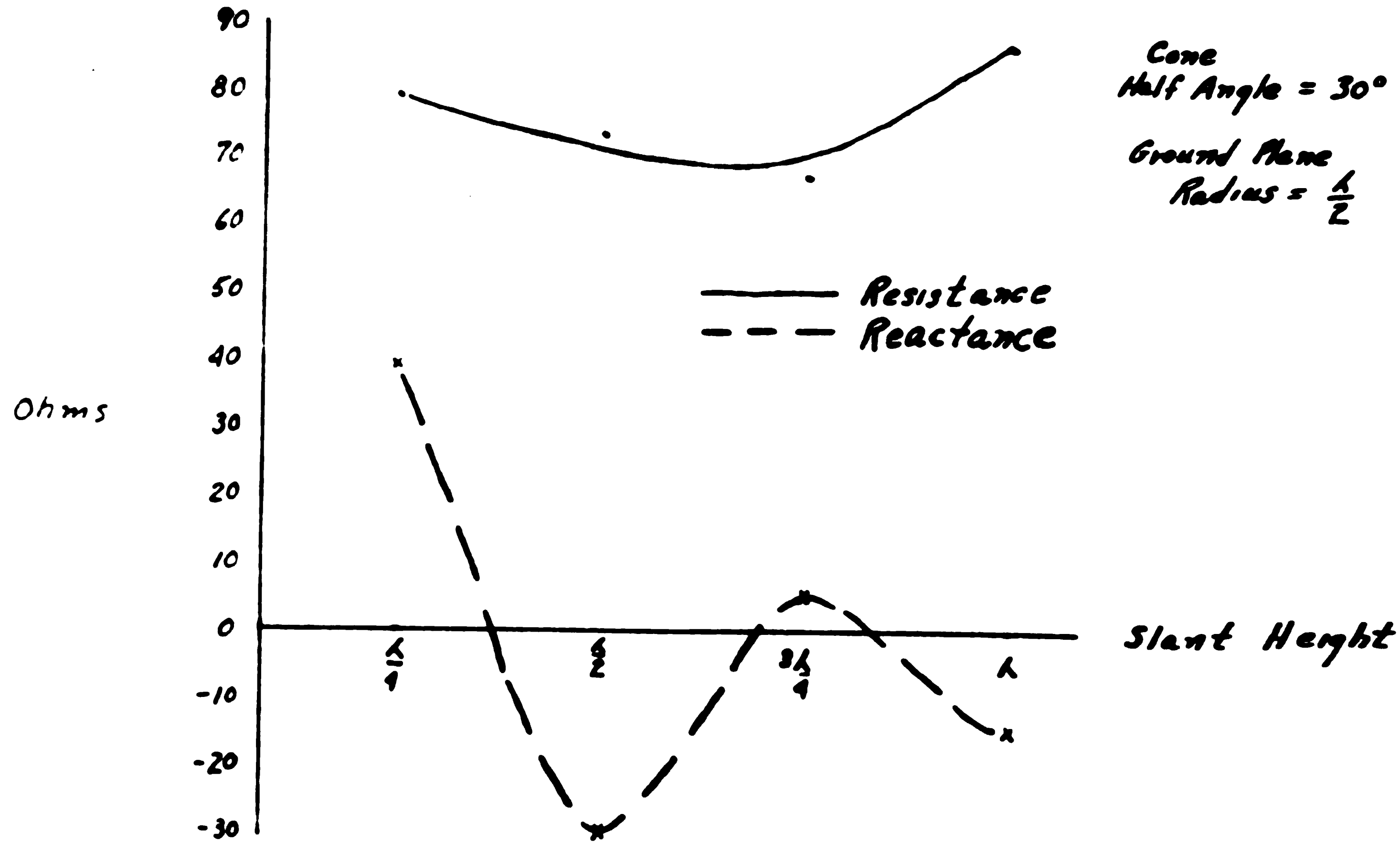

Figure 16

calculations were drawn on the graph of impedance vs. cone half angles. See Figure 17. The variations for small angles, as calculated by Smith, were included to show the sharp rise at small angles, indicating no valid comparison can be made with Schelkunoff's solution for thin cones, but showing the results are not incompatible.

The resistance components of the input impedance show the same trend and agree very well over most of the range. At small angles the work of Smith indicated there is a maximum at some position between 5° and 20°. No conclusive data was taken in this range of angles. At angles larger than 70° the curve of measured values indicates that the resistive component of the input impedance of a disk cone approaches very small values. A cone having a half angle of 90° would be a disk. Since the apex of the cone touches the ground plane in the theoretical problem, a half angle of 90° degrees would result in a shorted termination. These two results are in agreement.

The close agreement of Smith's calculations and the measured values show that for these cone angles the effect of a finite ground plane on the resistive component is small. Since in either case the antenna is assumed to be a perfect conductor there are no

Impedance of Disk Cone Antenna vs Cone Half Angle

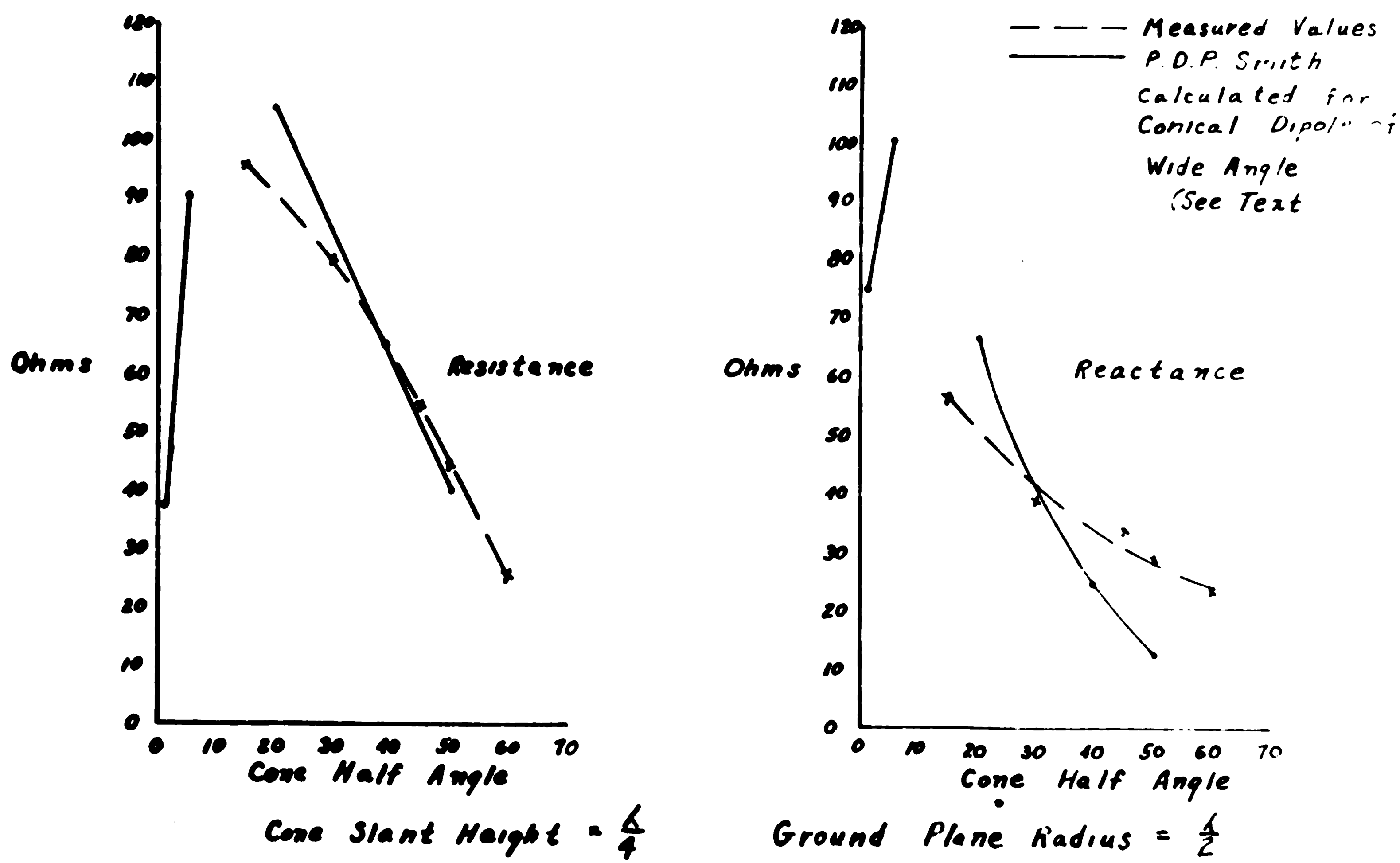

Figure 17

"Joule heat" losses. The resistive component is therefore the radiation resistance, and is directly proportional to the energy radiated. As a consequence, the radiated energy per unit of current input to the antenna is very nearly the same for a finite or an infinite ground plane.

The measured reactance decreases as the angle increases. This decrease is not as rapid as the decrease for a conical antenna calculated by Smith. By the same reasoning followed for the resistance at cone half angles of 90°, the reactance should decrease to zero at 90°.

It should be noted that the discrepancies between Smith's calculations and our measurements are greatest in the reactive component. Any discrepancy between the calculated and measured values of impedance should be due mainly to the fact that our ground plane is finite and not infinite, and that the base of our cone is flat and not spherically capped.

Variations due to changes in ground plane radius indicated oscillations in the impedance between a maximum and minimum approaching some limit at large ground planes. These variations have half period of one half a wavelength as shown in Figure 18. On the same graph the results of Meier and Summers are plotted. Their experimental data is for cylindrical dipoles with finite circular ground planes. No comparison of impedance values is intended since the cylindrical dipole

Disk Cone Impedance vs. Ground Plane Radius

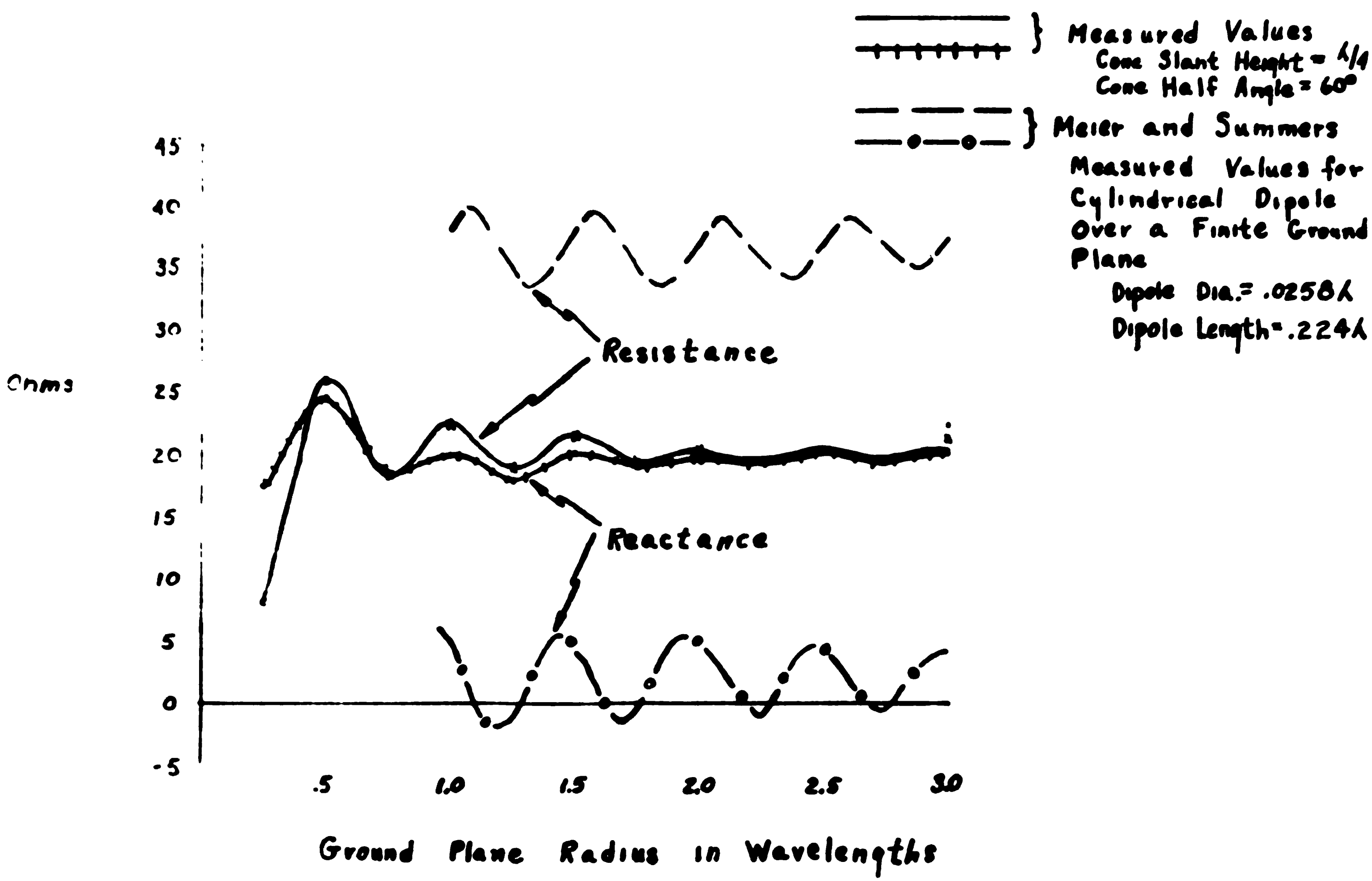

Figure 18

is similiar to the conical antenna of small angle discussed above. There is, however, qualitative agreement. Changes of the ground plane radius caused the resistive and reactive components of the input impedance to oscillate with a period of $\frac{\lambda}{2}$ for both types of antennas. For the disk cone the oscillations approached a limit more rapidly.

At very small ground planes the information was lacking so that the effects in that domain could not be given. At large ground planes the information was also incomplete.

The 60° cones of slant height $3/4\,\lambda$ and λ, were made hollow, with removable flat caps. They were placed over a ground plane with a radius of $\lambda/2$. No change was noted in the input impedance when the flat cap was removed.

The results show that a variation in any one of the parameters changed the input impedance. The largest variations of impedance were observed with changes in cone half angle, second largest with changes in slant height, and smallest with changes in ground plane radius. These graphs clearly show the general trends. There remain points which would be interesting to investigate, especially slant heights and ground plane radii less than one quarter of a wavelength, and the vicinity of zero reactive component in slant height variations.

The difficulties of measuring the input impedance of a disk cone have already been pointed out. With further investigations on the effect of surrounding objects, it might be found that the supporting line could be shortened. The conductors could be silver plated. Further improvements in the equipment such as detector, the oscillator, or any associated equipment, would make more accurate the measurements on the disk cone antenna input impedance.

BIBLIOGRAPHY

1. Schelkunoff, S.A., Theory of Antennas of Arbitrary Size and Shape, Proc. of I.R.E., 29, 493-521, 1941.

2. Schelkunoff, S.A., Electromagnetic Waves, D. Van-Nostrand Co., New York, 1943.

3. Schelkunoff, S.A., Principal and Complementary Waves in Antennas, Proc. of I.R.E., 34, 23-32, 1946.

4. Schelkunoff, S.A., General Theory of Symmetric Bi-conical Antennas, Jour. Appl. Phys., 22, 1330-1332, 1951.

5. Smith, P.D.P., The Conical Dipole of Wide Angle, Jour. Appl. Phys., 19, 11-23, 1948.

6. Eshbach, W.D.(Editor), Handbook of Engineering Fundamentals, Wiley and Sons Inc., New York, 1947.

7. Handbook of Chemistry and Physics, 31st Edition, Chemical Rubber Publishing Co., Cleveland, 1979, 1949.

8. Martin, R.L., A Ten Centimeter Oscillator, Unpublished M.S. Thesis, Michigan State College, 1948, 27 numb. leaves, 8 figures.

9. Mann, F.J.(Editor), Reference Data for Radio Engineers, 3rd Edition, Federal Telephone and Radio Corp., New York, 1949.

10. Meier and Summers, Measured Impedance of Vertical Antennas Over Finite Ground Planes, Proc. of I.R.E., 37, 609-616, 1949.

11. Ryder, J.D., Networks Lines and Fields, Prentice-Hall Inc., New York, 1949.

12. Terman, R.E., Radio Engineers Handbook, McGraw-Hill Book Co. Inc., New York, 1943.

13. Montgomery C.G., Technique of Microwave Measurements, McGraw-Hill Book Co. Inc., New York, 1947.

14. Bronwell, A.B. and Beam, R.E., Theory and Application of Microwaves, McGraw-Hill Book Co. Inc., New York, 1947.